Journal of Research in Science and Engineering (JRSE)
ISSN: 1656-1996 Volume-7, Issue-1, January 2025
DOI: 10.53469/jrse.2025.07(01).11

Experimental Investigation of Hybrid 3D Jute/Basalt Woven Composites Subjected to Low-velocity Impact Test

Jiaxuan Wang, Yiwei Ouyang, Ying Chai, Yao Song, Xiaozhou Gong*

School of Textile Science and Engineering, Wuhan Textile University, Wuhan 430200, China
Correspondence Author

Abstract: ***The aim of this study was to estimate the effect of weft blending on low-velocity impact properties. Based on whether the jute fibers have undergone alkali treatment the fabrics are systematically classified into two categories, to examine its impact on the jute fiber. The weft mixing ratio is 1:1,1:3 and 1:5. These fabrics were then converted into composite materials utilizing Vacuum Assisted Resin Transfer Molding (VARTM). An instrumented drop hammer impact test setup was employed to investigate the effects of varying impact energies (10J, 20J, and 30J). The findings revealed a notable 27% enhancement in impact resistance following an increase in jute content. This augmentation can be credited to the high flexibility and strain rate of jute fibres, which serve to prevent sudden fractures in the hybrid composite materials. Subsequent to the alkali treatment of jute, the impact strength of the resulting composite material has been observed to enhance by a range of 11% to 15%. For a more profound comprehension of the damage mechanism, the damage behaviour of the composite material following impact was investigated under a three-dimensional optical microscope. The impact surface mainly shows the separation of the yarn from the matrix, and the non-impact surface shows the fracture and resin damage of the yarn.***

Keywords: Hybrid, Composites, Jute, Basalt, Low-velocity impact, Damage behavior**.**

1. Introduction

In comparison to traditional metallic materials, fibre-reinforced composites have been employed extensively across a range of fields, including automotive, aerospace, marine, and offshore, due to their advantageous combination of advantageous combination of reduced density, robust mechanical properties, and modulus characteristics [1-3]. In this family of materials, resin-based basalt reinforced composites are particularly prominent, which can be processed into a variety of composite forms, including plywood, knitted fabrics and advanced 3D woven composites [4-9]. Among the aforementioned reinforcement materials, 3D woven composites have become a particularly crucial component due to their advantageous combination of low weight, high-quality strength, and rigidity ratio [10].

However, it should be noted that 3D woven composites are extremely sensitive to impact damage [11]. It is inevitable that low-velocity impacts, such as those resulting from the dropping of tools, gravel or debris, will occur in the context of manufacturing and operational processes. Such damage can manifest itself in various forms such as cracking of the matrix, fracture of the fibres, debonding and delamination of the fibres, etc [12]. In severe cases, the structural strength may be significantly reduced, even by more than 70% [13-14]. These potential damages pose a major threat to structural safety [15]. The enhancement of the impact resistance of carbon fibre composites represents a pivotal area of investigation in contemporary research [16].

The process of fibre blending serves as a powerful technique to improve the durability and shock absorbance of composite materials [17-18]. Hybrid fiber composites, composed of two or more fibers reinforcing the same matrix [19], retain the advantages of single-fiber composites while introducing new mechanical properties through the addition of other fibers [20-21]. There were three common methods of blending; Interlaminar blending [22-24], which specifically refers to the inclusion of one type of fiber in each layer of the plywood; Sandwich blending [25]: a core layer of one type of fiber was sandwiched between two layers of another type of single fiber; and Intra-laminar blending [26-27], where different types of fibers were used with a change in the type of matrix involved. By adjusting the materials and blending methods, they can meet diverse application needs while effectively reducing costs [28]. These composites find applications in aerospace, automotive, and various engineering fields.

The traditional basalt fiber-reinforced composite possesses remarkable characteristics, including superior specific strength, excellent stiffness, lightweight properties, and outstanding cost efficiency [29]. Nevertheless, its limited toughness often results in uncontrollable brittle failure, necessitating an increase in the safety factor during structural design and ultimately diminishing the material's utilization benefits [30]. Conversely, jute fiber composites exhibit relatively high elongation at break and are cost-effective, albeit with lower mechanical properties such as strength and modulus [31]. By mixing basalt fiber with fiber with greater toughness to prepare fiber hybrid composite materials, gradual failure can be realized, which helps the composite structure maintain function even under overload, improve safety and reduce the safety factor in the design [32]. In fiber hybrid composites, low-strain fibers fail earlier, but high-strain fibers with higher failure strains can withstand the load, so they can maintain their overall integrity and delay failure.

Some researchers had commenced research on 3D woven hybrid materials. For example, Hayashi [33] was the first to identify the hybrid effect, demonstrating that the failure strain of carbon fibres in carbon/glass fibre hybrid reinforced composites was 40% higher than that of pure carbon fibre composites. Wang [34] studied the influence of Kevlar layer positioning (at a 1:1 mixing ratio) on the material's response

to low-velocity impacts. They also delved into the damage mechanism of carbon/aramid fiber composite laminates, emphasizing how the layer sequence affects damage propagation in both symmetric and asymmetric hybrid laminates. Hu [35] designed three laminates reinforced with varying amounts of Kevlar staple fibers and studied their impact resistance and damage identification when exposed to two distinct impact energies. Rhead [36] used a combination of C-scan and micro-CT methods to visualize the internal delamination damage in carbon fiber/glass fiber interlayer hybrid laminates after post-impact compression tests. Their findings showed that hybrid laminates can significantly reduce the spread of internal delamination damage, and the effectiveness of this hybrid effect on post-impact compression performance depends on the hybrid structure itself. Farzin Azimpour-Shishevan [37] proved that adding carbon/basalt fibers to epoxy resin composites notably boosts their mechanical properties and resistance to high temperatures. Tian Jin [38] looked into how the mixing and stacking structure of carbon/aramid composites affect the mechanical properties of composite laminates.

The aim of this study was to examine how weft blending affects the performance of composites under low-velocity impact. To achieve this, we designed and produced 3D woven composites with different blend ratios of basalt and jute in the weft. These composites were then tested using a drop hammer for low-velocity impacts. The tests generated curves for load-time, load-displacement, and load-energy, which helped us understand how the composites responded to impacts with varying blend ratios. Additionally, we used a 3D optical microscope to inspect damage patterns on both sides of the material, providing insights into the damage mechanisms under different impact energies.

2. Experimental

2.1 Material

The 800tex basalt continuous fiber were provided by Zhejiang Shijin Basalt fiber Co., Ltd., while the 1mm jute was sourced from Baitang Trading Co., Ltd. of Huimin County. The epoxy resin JC-03A and curing agent JC-03B were supplied by Hang mo Jia fa New Material, while the NaOH reagent was provided by Sinopharm Group Industry Co., Ltd.

2.2 Alkali Treatment

Experimental results [39-40] have shown that alkali treatment can significantly improve the interfacial properties of materials and increase the strength of composites. Therefore, in this study, jute was pretreated with alkali by soaking it in a 50 g/L sodium hydroxide solution for three hours. Subsequently, the jute fibers were rinsed with deionized water to remove the sodium hydroxide solution. The washed jute fibers were then dried in an oven at 80 ℃ for eight hours.

2.3 Production of 3D Woven Fabrics

Six different types of curved shallow-crossing linking fabric are studied. The warp is composed of basalt and the weft is blended from basalt and jute in ratios of 1:1, 1:3 and 1:5, respectively. Then jute was divided into two groups according to whether it was treated with alkali or not (As shown as Table 1). The weaving process was successfully completed by using semi-automatic fabric sample machine. The parameters are set as follows: The preset width of the fabric sample is 150mm and the warp and weft density is 24 pieces per cm. Six brown racks were used, each reed tooth plus eight yarns, for a total of 270 warp threads. Figure 1 shows schematic representation of the weft mixing of the yarn.

Table 1: Weft structure parameters

Sample	Warp	Weft	Hybrid ratio	Alkaline treatment
A	Basalt	Jute/Basalt	1:1	×
B	Basalt	Jute/Basalt	1:3	×
C	Basalt	Jute/Basalt	1:5	×
AA	Basalt	Jute/Basalt	1:1	√
BB	Basalt	Jute/Basalt	1:3	√
CC	Basalt	Jute/Basalt	1:5	√

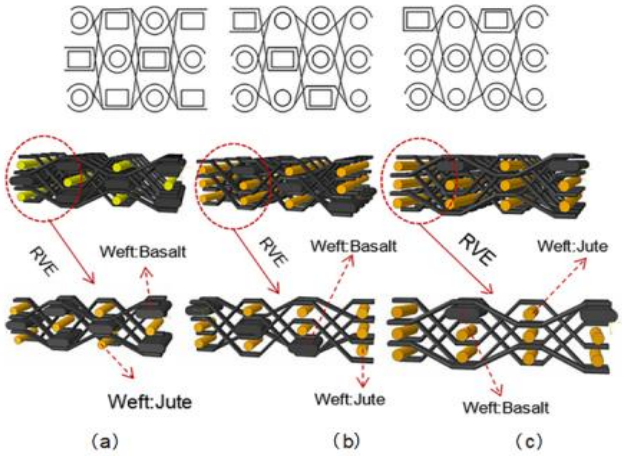

Figure 1: Diagram of mixed parameters (a)1:1 (b)1:3 (c)1:5.

2.4 Fabrication of Composite Samples

The vacuum-assisted resin transfer molding (VARTM) technique was used to inject epoxy resin (type JA-05, supplied by Jiafa Chemical Co., Ltd., China) into the fabric preforms. The curing process consisted of heating at 90°C for 2 hours, then at 110°C for 1 hour, and finally at 130°C for 4 hours (As shown as Figure 2). A low-velocity drop impact test was conducted in accordance with the standardised methodology set forth in the ASTM D7136/D7136M-15 standard. The samples were cut into rectangles measuring 75mm x 50mm using a cutting machine. (As shown as Table 2).The cross sections of composite materials with three hybrid ratios are shown in Figure 3.

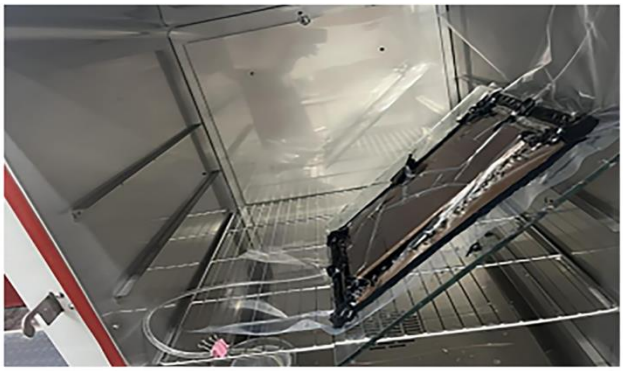

Figure 2: Schematic diagram of composite process

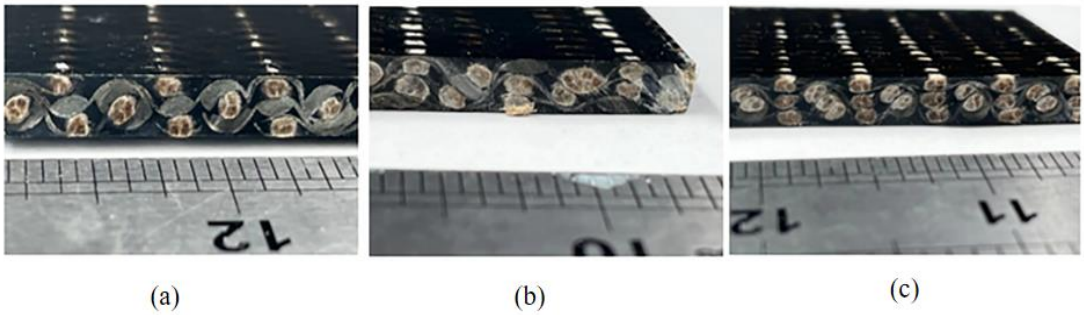

(a) (b) (c)

Figure 3: Cross section diagrams of composite materials
(a) The mixed ratio is 1:1 (b) The mixed ratio is 1:3 (c) The mixed ratio is 1:5

Table 2: Material specifications of the sample

Sample	Size(mm)	Mass /g	Thickness
A	75*50	33.70	5.06
B	75*50	33.40	5.17
C	75*50	33.66	5.22
AA	75*50	32.92	5.31
BB	75*50	32.87	5.37
CC	75*50	32.70	5.19

3. Test

3.1 Impact Performance Test

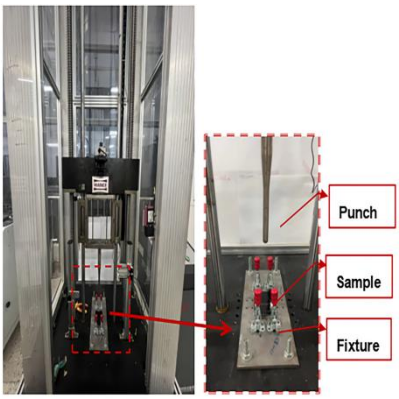

Figure 4: Instrument diagram for low-velocity impact of falling hammer

The low-velocity impact test was conducted utilising a DIT 302E instrumented drop impact tester (Illustrated in Figure 4), manufactured by the Shenzhen Wanshi Company. The requisite impact energies were attained by modifying the drop height of the punch. Quality of punches was 10 kg, and the diameter of the punch was 12.7 mm. The impact energies employed were 10 J, 20 J, and 30 J, with three samples tested for each energy level.

3.2 Microscopic Structural Characterization

Schematic diagrams of the microscopic damage patterns of each specimen after fracture were captured using a 3D microscope. The observation scale was set to 200μm to ensure adequate visualization of the damage features. Subsequently, the specimens were placed in the sample box, and photographs of the macroscopic damage patterns following fracture were taken for further analysis.

4. Discussion

4.1 Impact Response

Figure 5-6 shows the load-time curves for specimens A, AA, B, BB, C, and CC. From Figure 5(a), it is evident that the load profile of the specimen varies linearly with time. The curve can be separated into three distinct phases. In the first stage, a sawtooth increase in energy is observed as the punch makes contact with the specimen, resulting in the transfer of kinetic energy to the specimen. This results in deformation of the specimen and absorption of energy. The degree of jagged shaking increases in proportion to the amount of damage to the specimen. In the second stage, the curve continues to rise as the fibres take the brunt of the load, although the jerky variations become less pronounced. When the maximum displacement is reached and the punch stops, it has transferred all its kinetic energy to the specimen. In the third stage, the punch appears to rebound or continue to fall after reaching its maximum displacement.

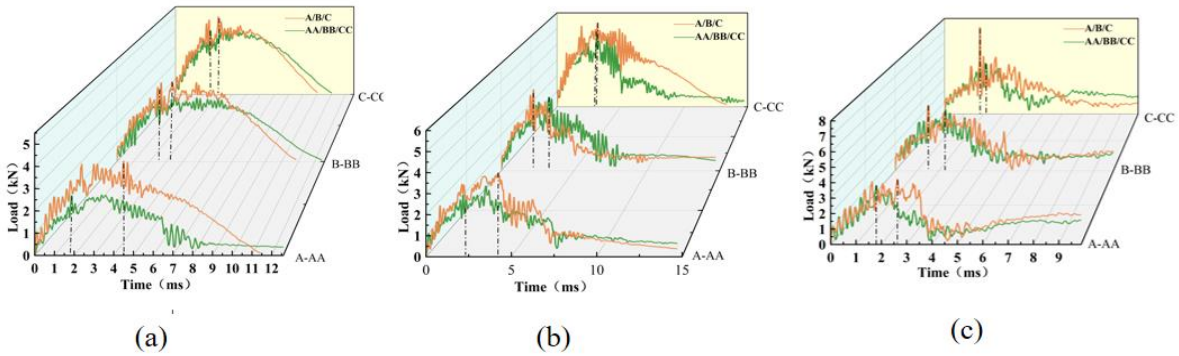

(a) (b) (c)

Figure 5: Load-time curve of impact process
(a) Load-time curve of 10J (b) Load-time curve of 20J (c) Load-time curve of 30J.

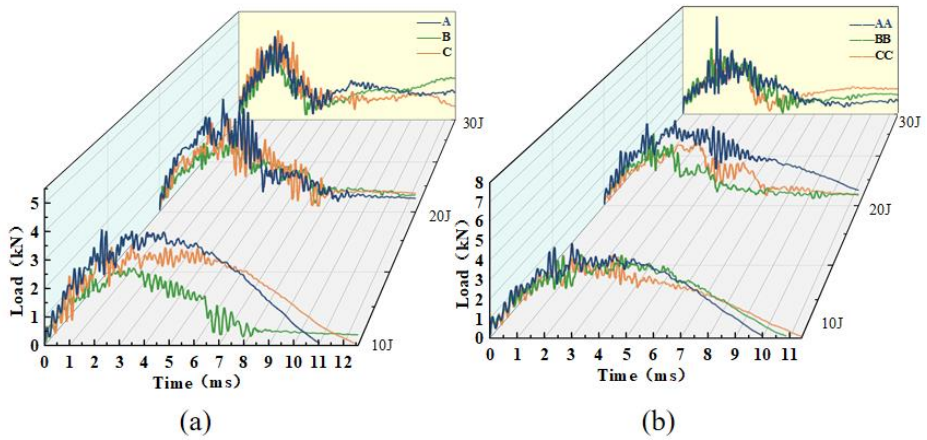

(a) (b)

Figure 6: Load-time curve of impact process
(a) Load-time curves of A-B-C at different energies (b) Load-time curves of AA-BB-CC at different energies

The material exhibited increasing stability under impact, as evident in Figure 6. This enhanced stability is primarily attributed to the good ductility and toughness of jute fibers, which effectively mitigate fiber fracture. As the proportion of jute fibers in the specimen gradually increased, the fluctuations in the curve became progressively smaller. The treated-jute specimens, as depicted in Figure 9(c), exhibited peak loads that were approximately 11-15% higher than their untreated counterparts under the same impact energy. Moreover, the duration of the impactor's contact with the specimens was extended. Referring to Figure 6(b), it is apparent that at equivalent energy levels, the peak loads of the AA, BB, and CC specimens surpassed those of the A, B, and C specimens by roughly 27%. This finding suggests that incorporating alkali-treated jute into the basalt composite material, subsequently utilized as a weft yarn, enhances the material's overall impact resistance. In addition, the reduction in surface impurities of the jute fibres improves the interfacial bonding between the jute and the resin, which ultimately improves the mechanical properties of the jute/basalt composite. As a result, the overall mechanical properties of the composite are improved. Figure 7-8 illustrates the load-displacement curves of specimens A, AA, B, BB, C, and CC subjected to three distinct impact energy levels: 10J, 20J, and 30J. Typically, three primary criteria are employed to assess composites under impact conditions: rebound, penetration, and perforation.

The load-displacement curve patterns can be categorized into closed and open types, each representing different stages of impact on the composite panel. In the closed type, rebound occurs when the kinetic energy of the punch was minimal, causing the punch to bounce back from the surface of the panel. Penetration, on the other hand, describes the transitional phase between rebound and perforation, where in the kinetic energy gradually increases, leading to the panel being on the brink of being penetrated. Finally, perforation happens when the kinetic energy reaches a critical value, and the punch completely penetrates the composite panel, with no remaining energy for rebound [40].

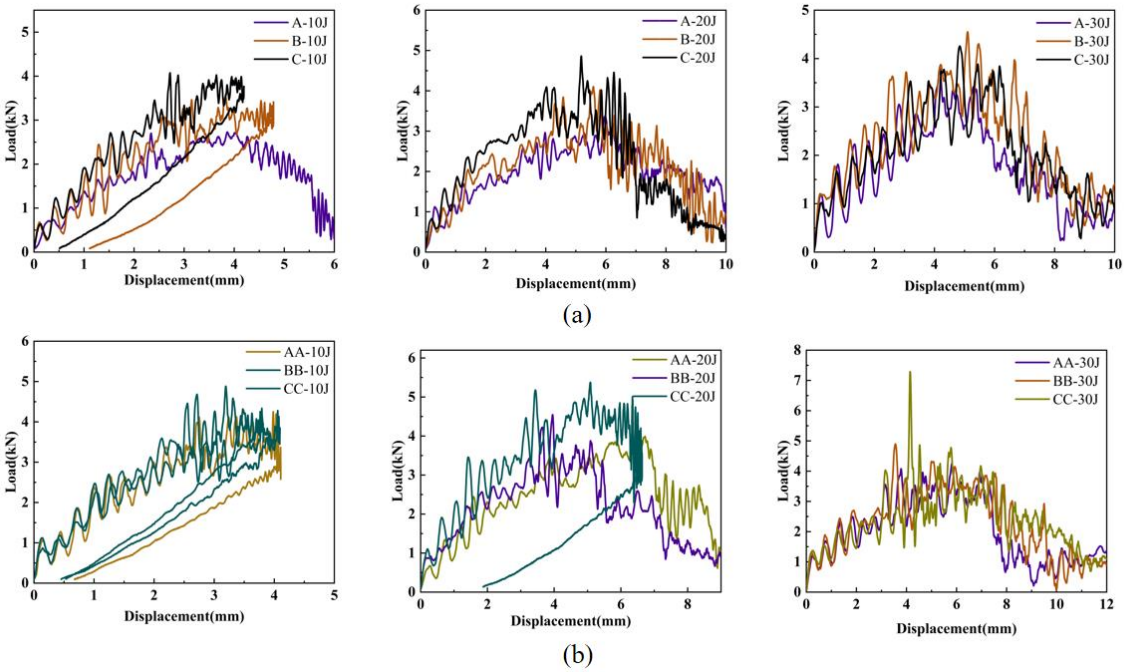

Figure 7: Load-displacement curve of impact process
(a) Load-displacement curve of A-B-C at different energies (b) Load-displacement curve of AA-BB-CC under different energies

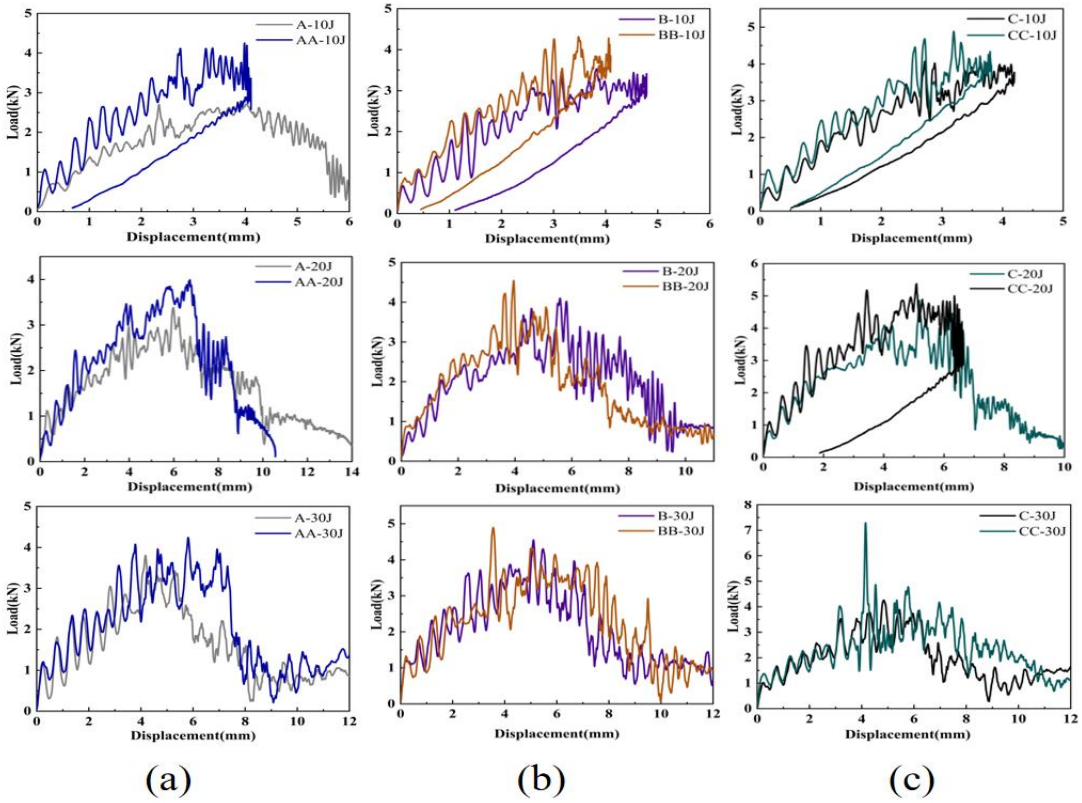

Figure 8: Load-displacement curve of impact process
(a) Load-displacement curve of A-AA at different energies (b) Load-displacement curve of B-BB under different energies
(c) Load-displacement curve of C-CC at different energies

When the punch makes contact with the composite panel, the load initiates a rising trend, albeit with a slight decrease at times, which are attributed to the generation of initial damage such as matrix cracks within the composite panel. As matrix cracks expand, along with fiber damage and delamination, the load increases until reaching its peak, after which the punch begins to rebound. As impact energy escalates, the curve's fluctuating strength intensifies gradually, which leads to a sudden drop in load in the vicinity of the peak load.

Continuing the impact process, the curve exhibits a significant decrease in stiffness upon surpassing the material load threshold. This decline in stiffness persists as the impact progresses. The curve's fluctuations become more pronounced with increasing impact energy due to the expanding stress wave, which induces initial damage within the laminate. The expansion of matrix and fiber damage, along with interlayer interface damage, creates irregular gaps within the laminate, destabilizing stress wave transmission and resulting in strong fluctuations in the curve.

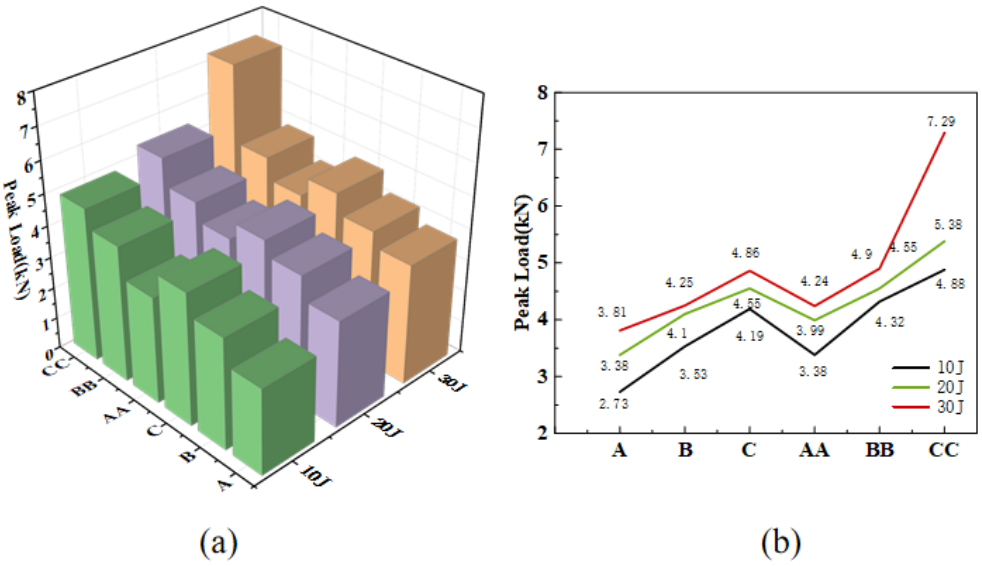

Figure 9: Comparison of the maximum load
(a) Comparison of the maxium load under different structure (b) Comparison of maxium loads of samples under different energies

Upon impact, specimen A tilted over at 10J (Figure 8(a)), while specimen C remained in a state of punch rebound after receiving an impact force of 20J (Figure 8(c)). This indicates that specimenn C was more resistant to impact than specimen A. Furthermore, the maximum load of A was higher than that of specimen C when the impact energy was 10J (Figure 9(c)). At identical impact energy and weft, the maximum load of the specimen increases with the increase of jute ratio (Figure 9(c)). The peak load at a mixing ratio of 1:3 was 11% higher than that at a mixing ratio of 1:1. This was because the specimen received the impact, with the surface layer of basalt being the first to experience it. However, basalt was brittle, so the introduction of jute enabled the impact to be distributed to the ductile jute layer in a gradual manner, thus enhancing the impact resistance effect.

Figure 10-11 show the absorbed Energy-time curves for different specimens. The specimen undergoes punching to carry out impact work, which entails matrix cracking, fiber extraction, and the dissipation of absorbed energy, leading to the creation of irreversible plastic damage. Additionally, some of the unabsorbed energy was converted into elastic deformation energy. In the three distinct energy impact scenarios, specimens AA, BB, and CC demonstrated low energy absorption, consequently leading to more pronounced specimen destruction.

At an impact energy of 10J, the curves of each specimen show a rising and then falling trend, followed by a rebound as the punch makes contact with the specimen. (Figure 10(a)). All else being equal, the specimen with the 1:5 mixing ratio showed the best energy absorption after impact, corresponding to a lower level of damage (Figure 11(c)). This is because the jute fiber's elongation at break and toughness are better. When subjected to external forces, the fiber deformation will be greater; therefore, the higher the jute fiber content, the better the energy absorption effect.

However, when the impact energy increases to 20 J, the CC specimen still shows a rebound tendency, while the other specimens tend to stabilize after reaching the peak value, with some exhibiting intrusion after the impact (Figure 10(b)). When the impact energy rises to 30 J, specimens A, B, and C fracture, with no excess energy for rebound (Figure 10(c)). AA, BB, and CC exhibit invagination. It can be observed that alkali-treated jute enhances the impact strength of the composite.

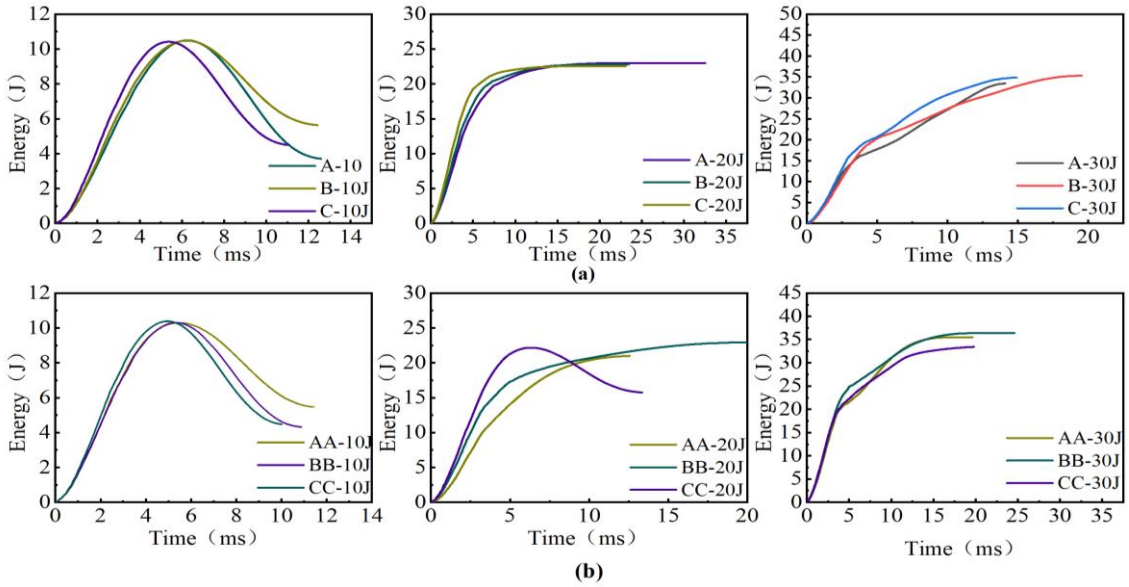

Figure 10: Energy-time curve of impact process
(a) Energy-time curves of sample under 10J (b) Energy-time curves of samples under 20J
(c) Energy-time curves of samples under 30J

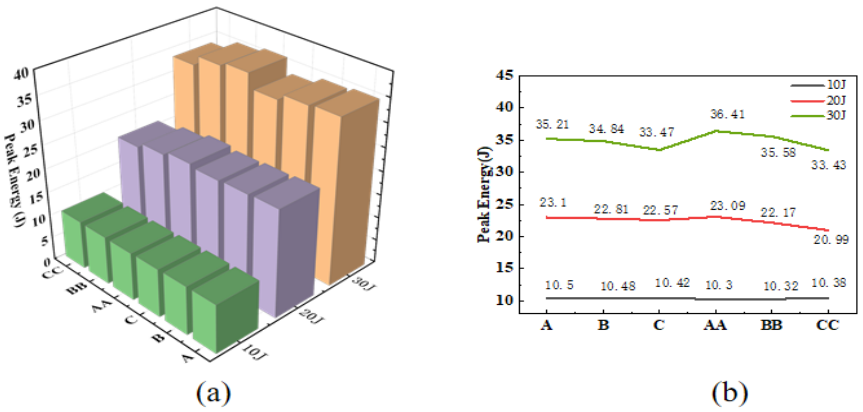

Figure 11: Comparison of the peak energy.
(a) Comparison of the peak energy under different structure (b) Comparison of peak energy under different energies

4.2 Damage Morphologies

The most common forms of damage observed in low-velocity impact specimens are matrix cracking, fiber fracture and fiber pull-out. As illustrated in Figure 12, the damage morphology diagrams of six specimens show a zigzag pattern before and after three different mixing ratios and jute treatments. However, the damage morphology and the degree of damage observed in these specimens vary. When the impact energy is 10J, a small amount of matrix cracking and crack damage is observed. Furthermore, no fiber damage is observed on the front of specimens B, C, AA, BB, and CC. A slight break in the resin occurs on the backside of A, resulting in a small quantity of fiber becoming detached.

When the impact energy reached 20 J, simultaneous impact processes occurred on both sides of the warp yarn in specimens A, B, C, AA, and BB. Subsequently, the wave-like flexure bent downward, facilitating contact between the punch and the specimen. Stress concentration during the bending of the specimen led to damage on its upper surface. The damage recorded on the impact side and non-impact side of the CC specimen was comparable to that observed at an impact energy of 10 J, but the extent of damage and the area of damage were greater. At an impact energy of 30 J, specimens A, B, and C suffered complete rupture, with fiber bundles fracturing and being extracted from the matrix. In contrast, the other specimens did not fracture completely, and specimen CC exhibited the least damage. Based on these findings, it can be inferred that post-treatment of jute enhances the low-velocity impact performance of composites to a certain extent.

The mixing ratios used in the manufacture of materials affect their impact properties. Hybrid fiber reinforced composites demonstrate a distinctive effect, termed the hybrid effect. The failure process in these composites is progressive; when stress is applied in the fiber direction, the more brittle fibers fracture prior to the ductile fibers. The basalt fibers, positioned at the surface due to their superior strength, generate a notable interfacial impact that propagates to the adjacent jute fibers. Since basalt fibers possess greater strength than jute fibers, they absorb more energy and initiate cracks when exposed on the surface. The ductility of jute fibers proves beneficial as they envelope the inner layer of basalt fibers, thereby preventing visible surface cracks and avoiding the occurrence of carbon fiber filament avalanches.

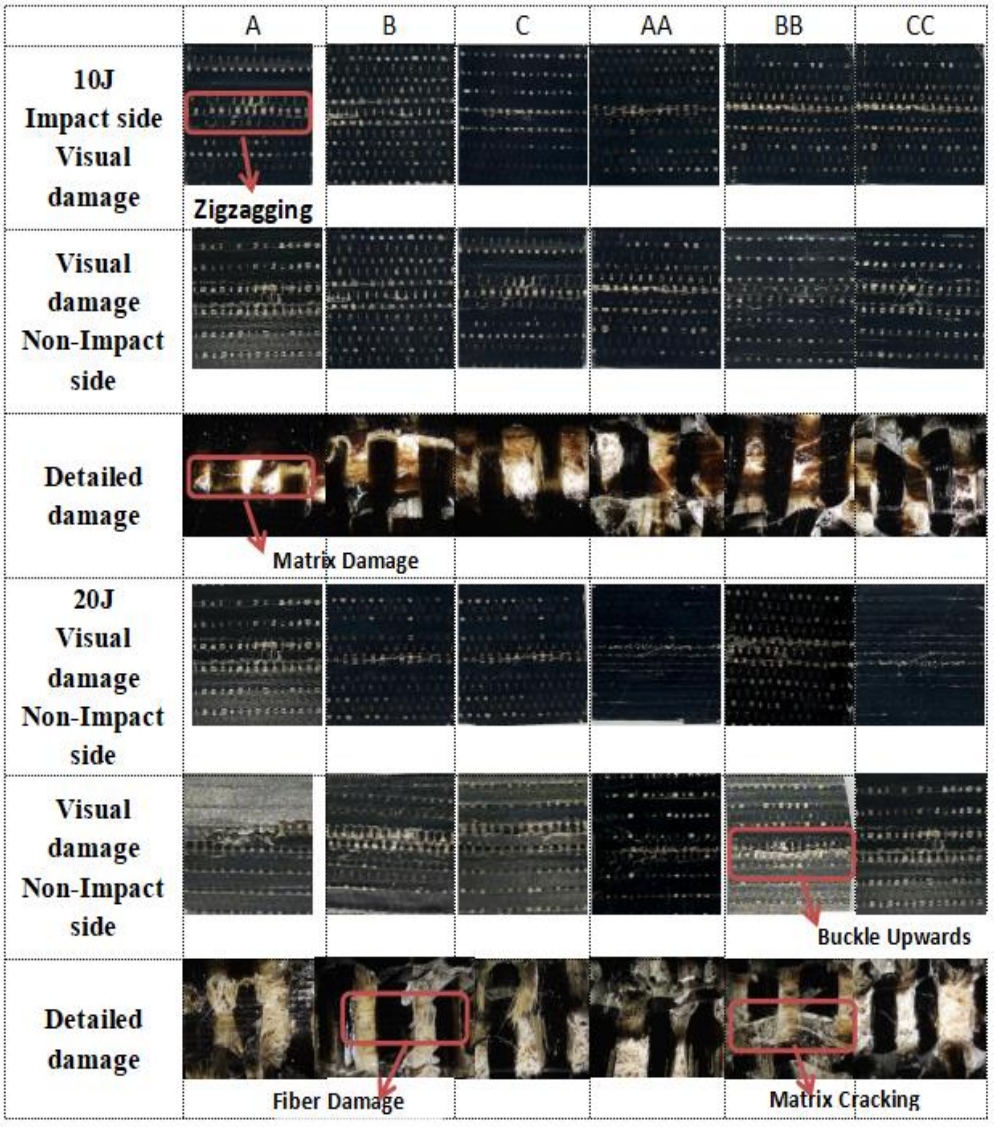

Figure 12: Damage mrophology

5. Conclusion

This study evaluates the dynamic mechanics of 3D woven composites subjected to low velocity impact, with the primary objective of assessing the effectiveness of jute-basalt hybridisation in enhancing the damage resistance of these composites. In this study, curved shallow-crossing linking 3D woven composites with weft mixing ratios of 1:1, 1:3 and 1:5 were considered. The main findings of the study are summarised below:

(1) The incorporation of alkali treated jute fibres significantly improved the impact performance of the hybrid composites, with an improvement of between 11% and 15%. This improvement can be attributed to the effect of the alkali treatment on the jute, suggesting that the impact resistance of jute composites is to some extent enhanced by the previous alkali treatment.

(2) The hybridisation effect in improving the impact strength of the composites became more pronounced as the impact energy increased from 10 J to 20 J and 30 J. Under identical impact energy levels, a higher content of jute fibers led to a higher peak load capacity of the composite material. The introduction of jute fibers mitigated catastrophic failure under tensile loads, transforming the fracture mode into a ductile fracture characterized by significant plastic deformation.

(3) As the impact energy escalated, the severity of material damage increased correspondingly. At lower As the energy level increased, yarn damage became more prevalent, leading to resin matrix withdrawal and ultimate composite failure.

References

[1] Sun, Guangyong, et al. "Energy absorption mechanics and design optimization of CFRP/aluminium hybrid structures for transverse loading," International Journal of Mechanical Sciences, 150, pp. 767-783, 2019.

[2] Zhou, Jianwu, et al. "Low-velocity impact behavior and residual tensile strength of CFRP laminates," Composites Part B: Engineering, 161, pp. 300-313, 2019.

[3] Bajpai A, Kadiyala A K and Ó Brádaigh CM, “Introduction to Epoxy/Synthetic Fiber Composites”. Handbook of Epoxy/Fiber Composites, In: Mavinkere Rangappa S, Parameswaranpillai J, Siengchin S, Thomas S (eds.), Springer, Singapore, pp. 1-31, 2022.

[4] Sebaey, T. A., et al. "Damage resistance and damage tolerance of dispersed CFRP laminates: Effect of the mismatch angle between plies," Composite Structures, 101, pp. 255-264, 2013.

[5] Liv, Y. I., et al. "Experimental study into compression after impact strength of laminates with conventional and nonconventional ply orientations," Composites Part B: Engineering 126, pp. 133-142, 2017.

[6] García-Rodríguez, S. M., et al. "The effect interleaving has on thin-ply non-crimp fabric laminate impact response: X-ray tomography investigation," Composites Part A: Applied Science and Manufacturing, 107, pp. 409-420, 2018.

[7] Sasikumar, A., et al. "Effect of ply thickness and ply level hybridization on the compression after impact strength of thin laminates," Composites Part A: Applied Science and Manufacturing, 121, pp. 232-243, 2019.

[8] Liu, Haibao, Brian G. Falzon, and Wei Tan. "Experimental and numerical studies on the impact response of damage-tolerant hybrid unidirectional / woven carbon-fibre reinforced composite laminates," Composites Part B: Engineering, 136, pp. 101-118, 2018.

[9] Liu, Haibao, Brian G. Falzon, and Wei Tan. "Predicting the Compression-After-Impact (CAI) strength of damage-tolerant hybrid unidirectional/woven carbon-fibre reinforced composite laminates," Composites Part A: Applied Science and Manufacturing, 105, pp. 189-202, 2018.

[10] Liu, Jun, et al. "The impact performance of woven-fabric thermoplastic and thermoset composites subjected to high-velocity soft-and hard-impact loading," Applied Composite Materials, 26, pp. 1389-1410, 2019.

[11] Liu, Xiaochuan, et al. "Impact response and crashworthy design of composite fuselage structures: An overview," Progress in Aerospace Sciences, pp. 101002, 2024.

[12] Lila M K, Verma A and Bhurat SS Impact Behaviors of Epoxy/Synthetic Fiber Composite, Handbook of Epoxy/Fiber Composites. In: Mavinkere Rangappa S, Parameswaranpillai J, Siengchin S, Thomas S (eds) Springer, Singapore, pp. 1-18, 2022.

[13] Cai, Xuanming, et al. "Anti-penetration response and response mechanism of laminated structures made of different composite materials under impact load," Thin-Walled Structures, 199, pp. 111840, 2024.

[14] Czech, Kamil, and Mariusz Oleksy. "Innovative method for studying impact energy absorption of hybrid polymer composites used in the defence industry," Measurement, 230, pp. 114499, 2024.

[15] Seamone, Andrew, et al. "Low velocity impact and compression after impact of thin and thick laminated carbon fiber composite panels," International Journal of Solids and Structures, 292, pp. 112745, 2024.

[16] Marsh, George. "Aero engines lose weight thanks to composites," Reinforced Plastics, 56.6, pp. 32-35, 2012.

[17] Swolfs, Yentl, Larissa Gorbatikh, and Ignaas Verpoest. "Fibre hybridisation in polymer composites: A review," Composites Part A: Applied Science and Manufacturing, 67, pp. 181-200, 2014.

[18] Safri, Syafiqah Nur Azrie, et al. "Impact behaviour of hybrid composites for structural applications: A review," Composites Part B: Engineering, 133, pp. 112-121, 2018.

[19] Pai, Yogeesha, K. Dayananda Pai, and M. Vijaya Kini. "A review on low velocity impact study of hybrid polymer composites," Materials Today: Proceedings, 46, pp. 9073-9078, 2021.

[20] Hai, Nguyen Duc, et al. "Structural behavior of hybrid FRP composite I-beam," Construction and Building Materials, 24.6, pp. 956-969, 2010.

[21] Talib, AR Abu, et al. "Development a hybrid, carbon/glass fiber-reinforced, epoxy composite automotive drive shaft." Materials & Design, 31.1, pp. 514-521, 2010.

[22] Gul, S., et al. "An experimental investigation on damage mechanisms of thick hybrid composite structures under flexural loading using multi-instrument measurements,"

Aerospace Science and Technology, 117, pp. 106921, 2021.
[23] Özbek, Özkan, Ömer Yavuz Bozkurt, and Ahmet Erkliğ. "An experimental study on intraply fiber hybridization of filament wound composite pipes subjected to quasi-static compression loading," Polymer Testing, 79, pp. 106082, 2019.
[24] Dehkordi, Majid Tehrani, et al. "The influence of hybridization on impact damage behavior and residual compression strength of intraply basalt/nylon hybrid composites," Materials & Design, 43, pp. 283-290, 2013.
[25] Attia, M. A., M. A. Abd El-baky, and A. E. Alshorbagy. "Mechanical performance of intraply and inter-intraply hybrid composites based on e-glass and polypropylene unidirectional fibers," Journal of Composite Materials, 51.3, pp. 381-394, 2017.
[26] Attia, M. A., M. A. Abd El-baky, and A. E. Alshorbagy. "Mechanical performance of intraply and inter-intraply hybrid composites based on e-glass and polypropylene unidirectional fibers," Journal of Composite Materials, 51.3, pp. 381-394, 2017.
[27] Kazemi, M. Erfan, et al. "Investigating the roles of fiber, resin, and stacking sequence on the low-velocity impact response of novel hybrid thermoplastic composites," Composites Part B: Engineering, 207, pp. 108554, 2021.
[28] Swolfs, Yentl, Larissa Gorbatikh, and Ignaas Verpoest. "Fibre hybridisation in polymer composites: A review," Composites Part A: Applied Science and Manufacturing, 67, pp. 181-200, 2014.
[29] Wei, Bin, Hailin Cao, and Shenhua Song. "Degradation of basalt fibre and glass fibre/epoxy resin composites in seawater," Corrosion Science, 53, pp. 1426-431, 2011.
[30] Wu, Gang, et al. "Durability of basalt fibers and composites in corrosive environments," Journal of Composite Materials, 49.7, pp. 873-887, 2015.
[31] Martinschitz, Klaus J., et al. "Changes in microfibril angle in cyclically deformed dry coir fibers studied by in-situ synchrotron X-ray diffraction," Journal of materials science, 43, pp. 350-356, 2008.
[32] Czél, Gergely, and Michael R. Wisnom. "Demonstration of pseudo-ductility in high performance glass/epoxy composites by hybridisation with thin-ply carbon prepreg," Composites Part A: Applied Science and Manufacturing, 52, pp. 23-30, 2013.
[33] Hayashi, Tsuyoshi. "On the improvement of mechanical properties of composites by hybrid composition," Proc. 8th Intl. Reinforced Plastics Conf, pp. 149-152,1972.
[34] Wang, Mingling, et al. "Symmetric and asymmetric intercalation effect on the low-velocity impact behavior of carbon/Kevlar hybrid woven laminates," Composite Structures 297, pp. 115919, 2022.
[35] Hu, Yuan, Weiwei Liu, and Yaoyao Shi. "Low-velocity impact damage research on CFRPs with Kevlar-fiber toughening," Composite Structures, 216, pp. 127-141, 2019.
[36] Rhead, Andrew T., Shi Hua, and Richard Butler. "Damage resistance and damage tolerance of hybrid carbon-glass laminates," Composites Part A: Applied Science and Manufacturing, 76, pp.224-232, 2015.
[37] Azimpour-Shishevan, Farzin, Hamit Akbulut, and M. A. Mohtadi-Bonab. "Mechanical and thermal properties of carbon/basalt intra-ply hybrid composites. I. Effect of intra-ply hybridization," Fibers and Polymers, 21, pp. 2579-2589, 2020.
[38] Tian, Jin, et al. "Study on behavior and mechanism of low-velocity impact and post-impact flexural properties of carbon-aramid/epoxy resin laminated composites," Composite Structures, 300, pp. 116166, 2022.
[39] Aggarwal, Manu, and A. Chatterjee. "Alkali pre-treatment of jute yarns for reinforcement in epoxy composites," Indian Journal of Fibre & Textile Research, 47, pp. 309-317, 2022.
[40] Padmaraj N H, Chemical Modification and Fabrication of Epoxy/Synthetic Fiber Composites, Handbook of Epoxy/Fiber Composites, In: Mavinkere Rangappa S, Parameswaranpillai J, Siengchin, Thomas S (eds) Springer, Singapore, pp. 1-24, 2022.
[41] Zhou, L, et al. "Low-velocity impact properties of 3D auxetic textile composite," Journal of materials science, 53.5, pp. 3899-3914, 2018.